Acta Crystallographica Section B
Structural Science
ISSN 0108-7681

Orientational disorder in crystals of $(NH_4)_3MoO_3F_3$ and $(NH_4)_3WO_3F_3$

A. A. Udovenko* and N. M. Laptash

Institute of Chemistry, Far Eastern Branch of RAS, Pr. Stoletiya 159, 690022 Vladivostok, Russia

Correspondence e-mail: udovenko@ich.dvo.ru

Received 1 February 2008
Accepted 15 April 2008

Triammonium trioxotrifluoromolybdate $(NH_4)_3MoO_3F_3$ (I) and trioxotrifluorotungstate $(NH_4)_3WO_3F_3$ (II) were synthesized in a single-crystal form and their structures were refined by X-ray diffraction. These two isostructural compounds belong to the elpasolite-type structure (cubic system, space group $Fm3m$, $Z = 4$). O and F atoms are randomly distributed in two independent positions [24(e) and 96(j)] of the cubic unit cell, and the central atoms and the ammonium cation containing N2 are shifted from the symmetry centers into the 32(f) position. As a consequence, O and F atoms in the equilibrium structure were identified on a local scale by the metal–ligand distance and hydrogen atomic coordinates of the disordered ammonium cation $N2H_4$ were determined. The slightly compressed MX_6 (M = Mo, W; X = O, F) octahedron has a *fac* configuration with the central atom shifted toward the face occupied by three O atoms. The true geometry of this polyhedron permits us to explain the observed vibrational spectra of the compounds examined and to eliminate the contradiction in interpretation of the vibrational spectra of $[MO_3F_3]^{n-}$ species reported in the literature. Both complexes reveal a dynamic disordering: the $[MX_6]^{3-}$ anions are disordered on 48 equivalent orientations and the $N2H_4$ groups have eight orientations.

1. Introduction

One of the important strategies for synthesizing new polar materials with a range of useful physical properties including pyroelectricity, ferroelectricity, piezoelectricity and second-harmonic generation (SHG) is to use inherently polar or non-centrosymmetric anions, particularly the strongly polar *fac*-$MO_3F_3^{3-}$ anion (Withers *et al.*, 2007; Maggard *et al.*, 2003). Crystallographic order of oxofluoride anions gives an opportunity to synthesize a non-centrosymmetric solid-state structure which is a potential candidate for use in new SHG materials (Heier *et al.*, 1999). In practice, however, many if not most transition metal oxofluoride compounds incorporating polar anions have turned out to be orientationally disordered giving rise to crystal structures where there is no resultant polarity and there appears to be no oxide/fluoride ordering at all, at least from a conventional three-dimensional crystallographic point of view (Withers *et al.*, 2007). Examples include $(NH_4)_3MoO_3F_3$ and $(NH_4)_3WO_3F_3$. The crystal structure of the first compound has not been refined since Pauling's time (Pauling, 1924) and the crystal structure of the second one was not determined until now in spite of it being known for more than 140 years and described by Marignac (Marignac, 1862, 1863) for the first time.

doi:10.1107/S0108768108010288

The search for direct evidence of oxygen/fluorine (O/F) ordering is complicated for any of the common diffraction techniques owing to the similarity in the scattering power of O and F. Withers *et al.* (2007) obtained the evidence of local O/F ordering for some relatively simple, high-symmetry, 'disordered' transition-metal oxofluorides *via* the analysis of highly structured diffuse intensity distributions, including a combination of structured diffuse scattering and Monte Carlo modeling for $K_3MoO_3F_3$ (Withers *et al.*, 2003).

In this paper, using common X-ray diffraction, we demonstrate the first examples of local O/F ordering in the highly disordered ammonium oxofluoroelpasolites $(NH_4)_3MoO_3F_3$ and $(NH_4)_3WO_3F_3$ that explain their experimental vibrational spectra and eliminate a contradiction in the interpretation of the vibrational spectra of $[MO_3F_3]^{n-}$ species reported in the literature.

2. Experimental

2.1. Synthesis

Both complexes $(NH_4)_3MoO_3F_3$ and $(NH_4)_3WO_3F_3$ were synthesized in single-crystal form. The starting materials (reagent grade) were used for the synthesis of the above compounds. Aqueous ammonium molybdate solution (or a solution of molybdic acid in ammonia) was mixed with a concentrated solution of NH_4F (40%). A large quantity of white precipitate appeared immediately, which was a mixture of $(NH_4)_3MoO_3F_3$ and $(NH_4)_2MoO_3F_2$. The solid was then dissolved in an aqueous solution of a small amount of HF with excess NH_4F. The solution was heated and hydrolyzed with NH_3 to pH = 7–8 when a solid reappeared, which was pure fine-crystalline $(NH_4)_3MoO_3F_3$. The larger crystals were obtained from the mother liquor under slow evaporation in air. The first portions of crystals were hexagonal plates. Further crystallizations gave octahedral single crystals. Both forms were used for structural determinations and refinement results on both crystals were identical.

Ammonium oxofluorotungstate $(NH_4)_2WO_2F_4$ served as a precursor for $(NH_4)_3WO_3F_3$. Two methods were used for the preparation of the precursor:

(i) Fluorination of tungstates with concentrated HF. We used ammonium *para*-tungstate.

(ii) Fluorination of tungsten trioxide WO_3, ammonium tungstate or calcium tungstate (scheelite) $CaWO_4$ with ammonium hydrogen difluoride, NH_4HF_2.

The initial components were mixed in a stoichiometric ratio and heated to 473 K, producing $(NH_4)_3WO_2F_5$. $CaWO_4$ was preferable as a starting material as it interacts faster with NH_4HF_2, even at room temperature.

$$CaWO_4 + 3.5NH_4HF_2 = CaF_2 + (NH_4)_3WO_2F_5 + 0.5NH_3 + 2H_2O$$

The cake was leached using water (solid:liquid = 1:4) and the mother liquor was filtered and slowly evaporated in air. Differently shaped single crystals (thick plates, prisms, isometric polyhedra) of $(NH_4)_2WO_2F_4$ were crystallized from saturated solutions.

$(NH_4)_3WO_3F_3$ was obtained from a hot solution of $(NH_4)_2WO_2F_4$ in excess NH_4F followed by the addition of aqueous NH_3 until a white product appeared during the process of stirring. Further crystallization from mother liquor gave larger octahedral single crystals which were suitable for structural determinations. Both $(NH_4)_3MoO_3F_3$ and $(NH_4)_3WO_3F_3$ were chemically analyzed. Anal.: calc. for $(NH_4)_3WO_3F_3$: NH_4 15.8, W 53.6, F 16.6; found: NH_4 15.8, W 53.3, F 16.5. Calc. for $(NH_4)_3MoO_3F_3$: NH_4 21.2, Mo 37.6, F 22.4; found: NH_4 21.2, Mo 37.8, F 22.0.

Ammonia was determined by the Kjeldahl method with a precision of ±0.3 mass %. Pyrohydrolysis at 673 K was used for the simultaneous determination of fluorine and the metal. 0.2–0.4 g of the sample were placed in a Pt boat and hydrolyzed in superheated steam over 2 h. HF was water absorbed followed by titration with $Th(NO_3)_4$, and the metal was analyzed gravimetrically by weighting MoO_3 or WO_3. The precision of fluorine and metal determination was ±0.5 mass %.

2.2. X-ray studies

Crystal structures of $(NH_4)_3MoO_3F_3$ and $(NH_4)_3WO_3F_3$ were determined at 570 (1) K using a Bruker SMART 1000 CCD diffractometer (Mo $K\alpha$ radiation, graphite monochromator). Data collection was carried out by ω scanning with a step size of 0.2° and an exposure time of 20 s per frame. Three groups of 906 frames each were collected at $\varphi = 0$, 90 and 180°, respectively, with the crystal–detector distance of 45 mm. Visible reflections disappeared above $\theta_{\max} = 30°$ which accounted for the relatively small number of independent reflections. Octahedral single crystals with an edge size of 0.25 mm were used. Larger crystals were imperfect.

Crystal structures of (I) and (II) with M (M = Mo, W) in position 4(a), N in 4(b) and 8(c) positions, and F(O) atoms in position 24(e) were solved by direct methods and refined by the least-squares method in anisotropic approximation with $R_1 = 0.0600$ and 0.0191 for (I) and (II), respectively. The location of the ligand atoms in the mixed 24(e) + 96(j) position lowered R_1 to 0.0454 and 0.0134, respectively. The additional structure refinement with M and N2 displaced from the symmetry centers reduced R_1 to 0.0291 and 0.0107 for (I) and (II), respectively, owing to atomic displacement from 4(a) and 4(b) positions into 32(f). Comparable refinement of the crystal structures of fluoroelpasolites $(NH_4)_3AlF_6$, $(NH_4)_3FeF_6$ and $(NH_4)_3GaF_6$ did not lead to any reducing of R by displacement of the corresponding atoms from the symmetry center, and the atoms were returned to their initial special positions.

The atomic coordinates of H1 and H2 atoms were taken from the crystal structure of $(NH_4)_3AlF_6$, where they were reliably localized from the electron density difference map, and atomic coordinates of H3 were determined geometrically. Coordinates and isotropic displacement parameters of all H atoms (H1, H2 and H3) were refined separately using limited reflections ($2\theta_{\max} = 46°$) with all fixed non-H atoms. The final structure refinement with fixed H atoms gave R_1 equal to 0.0174 and 0.0090 for (I) and (II), respectively. The same

Table 1
Crystal data and structure refinement for $(NH_4)_3MoO_3F_3$ (I) and $(NH_4)_3WO_3F_3$ (II).

	(I)	(II)
Crystal data		
Chemical formula	$F_3O_3Mo{\cdot}3NH_4$	$F_3O_3W{\cdot}3NH_4$
M_r	255.07	342.98
Cell setting, space group	Cubic, $Fm\bar{3}m$	Cubic, $Fm\bar{3}m$
Temperature (K)	297 (2)	297 (2)
a (Å)	9.1295 (3)	9.1563 (3)
V (Å^3)	760.92 (4)	767.64 (4)
Z	4	4
D_x (Mg m^{-3})	2.226	2.968
Radiation type	Mo $K\alpha$	Mo $K\alpha$
μ (mm^{-1})	1.74	15.07
Crystal form, color	Octahedron, colorless	Octahedron, colorless
Crystal size (mm)	0.33 × 0.25 × 0.17	0.33 × 0.25 × 0.17
Data collection		
Diffractometer	Bruker Smart 1000 CCD	Bruker Smart 1000 CCD
Data collection method	ω scans	ω scans
Absorption correction	Multi-scan	Multi-scan
$T_{\min}$	0.597	0.083
$T_{\max}$	0.756	0.184
No. of measured, independent and observed reflections	2016, 89, 85	2269, 83, 83
Criterion for observed reflections	$I > 2\sigma(I)$	$I > 2\sigma(I)$
$R_{\rm int}$	0.031	0.037
$\theta_{\max}$ (°)	30.7	29.8
Refinement		
Refinement on	F^2	F^2
$R[F^2 > 2\sigma(F^2)]$, $wR(F^2)$, S	0.017, 0.053, 1.24	0.009, 0.019, 1.20
No. of reflections	89	83
No. of parameters	18	18
H-atom treatment	Not refined	Not refined
Weighting scheme	$w = 1/[\sigma^2(F_o^2) + (0.0331P)^2 + 0.460P]$, where $P = (F_o^2 + 2F_c^2)/3$	$w = 1/[\sigma^2(F_o^2) + (0.0125P)^2]$, where $P = (F_o^2 + 2F_c^2)/3$
$(\Delta/\sigma)_{\max}$	0.042	0.032
$\Delta\rho_{\max}$, $\Delta\rho_{\min}$ (e Å^{-3})	0.17, −0.20	0.20, −0.19
Extinction method	*SHELXL*	*SHELXL*
Extinction coefficient	0.0417 (6)	0.00265 (4)

Computer programs used: *SMART* (Bruker, 1998*a*), *SAINT* (Bruker, 1998*b*), *SHELXTL*/*PC* (Sheldrick, 2008).

refinement procedure for the 24(e) ligand position led to $R1$ = 0.0580 and 0.0162, respectively.

The data collection and reduction as well as the refinement of the lattice parameters were performed using *SMART* and *SAINT-Plus* programs (Bruker, 1998*a*,*b*). All the calculations were performed with the *SHELXTL*/*PC* program (Sheldrick, 2008). Table 1[1] gathers the conditions of the diffraction experiment, crystallographic data and structure refinement for $(NH_4)_3MoO_3F_3$ and $(NH_4)_3WO_3F_3$. Interatomic distances and valence angles are presented in Table 2 and the hydrogen-bond parameters are given in Table 3. Further structural details can be obtained from the Fachinformationszentrum Karlsruhe, 763444 Eggenstein-Leopoldschaften, Germany [fax: (49) 7247-808-666; e-mail: crysdata@fiz-karlsruhe.de] on quoting the depository numbers CSD 418433 and 412987 for $(NH_4)_3MoO_3F_3$ and $(NH_4)_3WO_3F_3$, respectively.

2.3. IR and Raman spectra

The FT–IR spectra were recorded on a Shimadzu FTIR Prestige-21 spectrometer at ambient temperature in the range 400–4000 cm^{-1}. The resulting spectra after subtraction of the baseline were smoothed (Savitsky–Golay algorithm, 11 points) and fitted with Gaussian–Lorentzian functions using a commercially available program (Systat PeakFit). Below 400 cm^{-1}, the FT-IR spectra were recorded on an Equinox 55/S spectrometer.

The FT-Raman spectra of the samples were recorded with a RFS 100/S spectrometer. The 1064 nm line of an Nd:YAG laser (130 mW maximum output) was used to excite the sample. The spectra were recorded at room temperature.

3. Results and discussion

3.1. Crystal structures

The treatment of experimental results for (I) and (II) gave five possible space groups of the cubic symmetry: $Fm3m$ (No. 225), $F\bar{4}3m$ (No. 216), $F432$ (No. 209), $Fm3$ (No. 202) and $F23$ (No. 196). The same low R factors [0.0174 and 0.0.090 for (I) and (II), respectively] have been achieved in the first two groups so we decided on the higher symmetry group $Fm3m$. It should be noted that this space group is accepted for the most commonly known cubic elpasolites. Refinement in the remaining space groups was unstable with higher R factors. The ligand atoms in the $Fm3m$ group are statistically distributed in two positions 24(e) and 96(j). The preference of this 'mixed' (or 'split') position relative to 24(e) has been discussed in our previous paper (Udovenko *et al.*, 2003) concerning the orientational disorder in crystals of ammonium fluoroelpasolites. The location of the ligand atoms in the 24(e) position results in relatively high R values and large isotropic displacement parameters. In the structure solution of elpasolite $(NH_4)_3GaF_6$, fluorine is assumed to occupy the 192(l) position in the lattice with a site occupancy of 1/8 (Schwarzman, 1964). Quite recently, the MAS NMR findings showed this position to be subject to errors (Krahl *et al.*, 2008). The 192(l) position is not found in the structures of $(NH_4)_3MoO_3F_3$ and $(NH_4)_3WO_3F_3$.

Pauling was puzzled (Pauling, 1924) as to how the MO_3F_3 groups can be arranged in a manner completely concordant with the symmetry of the larger unit. Today we can understand how. We carried out the additional refinement of the struc-

---

[1] Supplementary data for this paper are available from the IUCr electronic archives (Reference: BP5011). Services for accessing these data are described at the back of the journal.

Table 2
Bond lengths (Å) and angles (°) in the structures of (I) and (II).

	(I)	(II)		(I)	(II)
M—O1	1.667 (1)	1.732 (2)	N1—X2† ×4	2.895 (1)	2.914 (2)
M—O2	1.684 (2)	1.762 (2)	N2—F1	2.597 (2)	2.596 (2)
M—O2A	1.802 (2)	1.830 (2)	N2—F2	2.643 (2)	2.644 (2)
M—F1	2.027 (1)	1.955 (2)	N2—F2′	2.705 (2)	2.707 (2)
M—F2	2.038 (2)	1.978 (2)	N2—O1	2.891 (2)	2.903 (2)
M—F2A	2.136 (2)	2.040 (2)	N2—O2	2.934 (2)	2.948 (2)
X1—X2 ×8	2.635 (1)	2.640 (2)	N2—O2′	2.990 (2)	3.005 (3)
X2—X2 ×4	2.684 (2)	2.681 (3)			
O1—M—O2	103.67 (1)	98.14 (1)	F2—M—F2A	80.00 (1)	83.69 (1)
O1—M—O2A	98.79 (1)	95.60 (1)	F2A—M—O2A	85.48 (1)	87.54 (1)
O1—M—F2	90.11 (1)	90.44 (1)	O2A—M—O2	100.60 (1)	96.56 (1)
O1—M—F2A	86.82 (1)	88.44 (1)	O2—M—F2	91.77 (1)	91.40 (1)
F1—M—F2	80.85 (1)	84.30 (1)	O1—M—F1	163.88 (1)	170.13 (1)
F1—M—F2A	78.52 (1)	82.69 (1)	O2—M—F2A	166.77 (1)	171.85 (1)
F1—M—O2	90.01 (1)	90.36 (1)	O2A—M—F2	162.52 (1)	169.21 (1)
F1—M—O2A	86.80 (1)	88.38 (1)			

† X = O(F).

Table 3
Hydrogen-bond lengths (Å) and angles (°) for (I) and (II).

	H···X		N···X		N—H···X	
N—H···X	(I)	(II)	(I)	(II)	(I)	(II)
N1—H1···F2 ×2	2.21	2.17	2.895 (1)	2.914 (2)	144	143
N1—H1′···O2 ×2	2.21	2.17	2.895 (1)	2.914 (2)	144	143
N2—H2···F1	1.78	1.73	2.597 (1)	2.596 (2)	165	166
N2—H2′···F2	1.89	1.83	2.643 (1)	2.644 (3)	151	151
N2—H2″···F2′	1.89	1.83	2.705 (1)	2.707 (2)	168	168

tures, including the displacement of the central M atom into the 32(f) position and reconstructed a separate orientation of MX_6. A coordination polyhedron with different M—X distances was obtained as a result. Three short distances correspond naturally to the M—O bonds and three others correspond to the M—F bonds (Fig. 1, Table 2). The polyhedron has a *fac* configuration (three O atoms and three opposite F atoms occupy an octahedral face). It should be noted that one M—O distance is significantly longer than the other two (1.80 and 1.67 Å for Mo elpasolite and 1.83 and 1.73–1.76 Å for W elpasolite, respectively). The coordination polyhedra in (I) and (II) are slightly compressed along the X1—X1 axis (on 0.14 and 0.12 Å, respectively). The M atoms are shifted on 0.314 and 0.194 Å for (I) and (II), respectively, from the octahedral center toward the face occupied by O atoms.

The arrangement of the ligand atoms in two independent positions [24(e) + 96(j)] leads to six equivalent orientations of MX_6 (two orientations along each axis of the unit cell). Taking into account the identification of O and F atoms, the number of MX_6 equivalent orientations rises to 48 (16 orientations along each axis, Fig. 2). Fig. 3 demonstrates one of the possible orientations of the $(NH_4)_3MO_3F_3$ structure that reflects the possible configuration of its domain. Three variants of the $[MO_3F_3]$ mutual arrangement in a crystal can be imagined.

(i) All octahedra are randomly re-orientating which is unlikely because of their coordinated movements owing to hydrogen bonding through ammonium cations (see below).

(ii) Being connected by the elements of the merohedral $Fm3m$ symmetry, all octahedra are simultaneously moving by jumping from one to another possible orientation. Such a structure should reveal a relatively large dipole moment (see Fig. 3) that is in fact not realised.

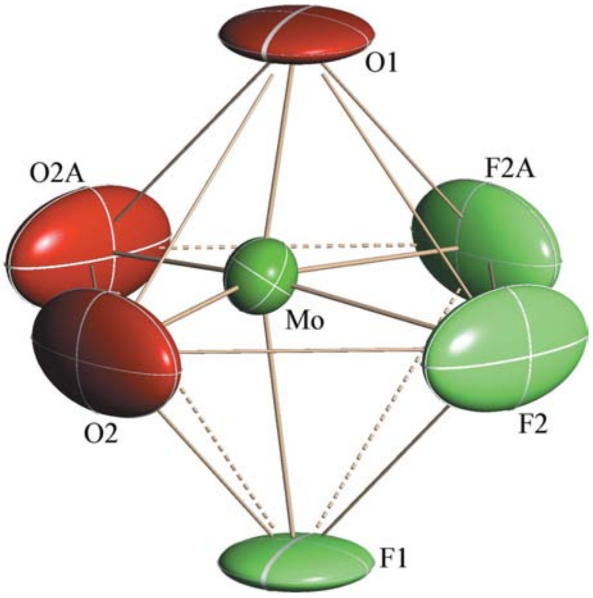

Figure 1
$[MoO_3F_3]^{3-}$ octahedron in the crystal structures of $(NH_4)_3MoO_3F_3$ ($[WO_3F_3]^{3-}$ octahedron is similar).

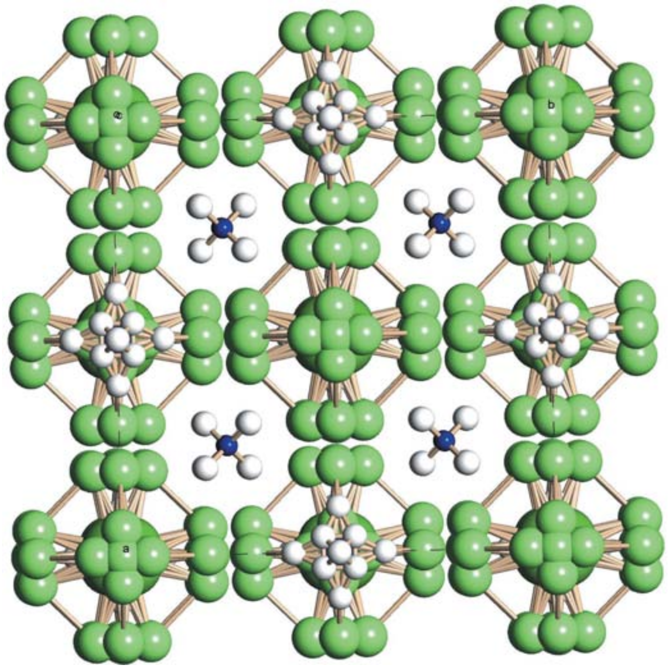

Figure 2
Disordered structure of $(NH_4)_3MO_3F_3$. Light-green spheres: X (O, F) atoms; dark-green spheres (under light-green ones): M atoms; blue spheres: N atoms; white spheres: H atoms.

(iii) Most likely, a single crystal is formed by a number of differently oriented microdomains related by the *Fm*3*m* symmetry elements.

The spatial orientation of each separate microdomain changes by jump in accordance with interrelated movement of octahedra and ammonium cations. The total dipole moment of the structure remains at zero for each point of time. Recent MAS NMR experiments on $(NH_4)_3GaF_6$ elpasolite indicate that both NH_4^+ ions and $[GaF_6]^{3-}$ octahedra undergo rapid reorientation rotations (Krahl *et al.*, 2008) that support our suggestion on the dynamic nature of disorder in all ammonium fluoroelpasolites.

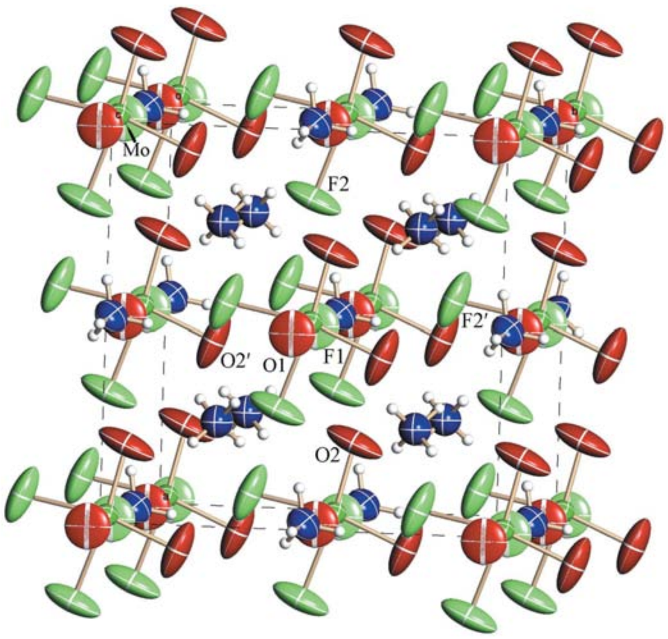

Figure 3
One of the possible orientations (domains) of the $(NH_4)_3MoO_3F_3$ structure [domain of $(NH_4)_3WO_3F_3$ is similar].

N atoms are located in two positions of structures (I) and (II). $N1H_4$ groups occupy tetrahedral interstices formed by MX_6 octahedra, while $N2H_4$ groups are placed in octahedral interstices formed by MX_6. The electron density peaks around N1 and N2 appear respectively as a regular tetrahedron and octahedron with reasonable N—H distances in the electron-density difference map. The octahedron around N2 indicates disorder of the $N2H_4$ group as has been found in other ammonium fluoroelpasolites (Udovenko *et al.*, 2003). The situation is very similar to dynamic orientational disorder in the NH_4I crystal (Seymour & Pryor, 1970; Paasch *et al.*, 1996), where several possible models of disorder were proposed. These models are different by the number of equal N—H$\cdots$I bonds. In our case, however, the regular octahedral environment of the ammonium tetrahedron is absent (Table 2) if the equilibrium anionic packing of $(NH_4)_3MO_3F_3$ (Fig. 3) is taken into consideration. Three H2 atoms of the $N2H_4$ group form three hydrogen bonds under tetragonal angles with the nearest F atoms (Table 3) owing to the displacement of N2 from the symmetry center, and the fourth H3 atom lies on a threefold axis in the 32(*f*) position (Fig. 4) and does not form a hydrogen bond. This disorder (Fig. 5) gives eight equivalent orientations of the $N2H_4$ group, and each vertex of the observed octahedron is the electron density superposition from four H2 atoms of these eight orientations. Thus, the disorder in the ammonium fluoroelpasolites investigated is of dual nature: both the central (*M* and N) and ligand atoms (O/F and H) are statistically distributed in the corresponding positions.

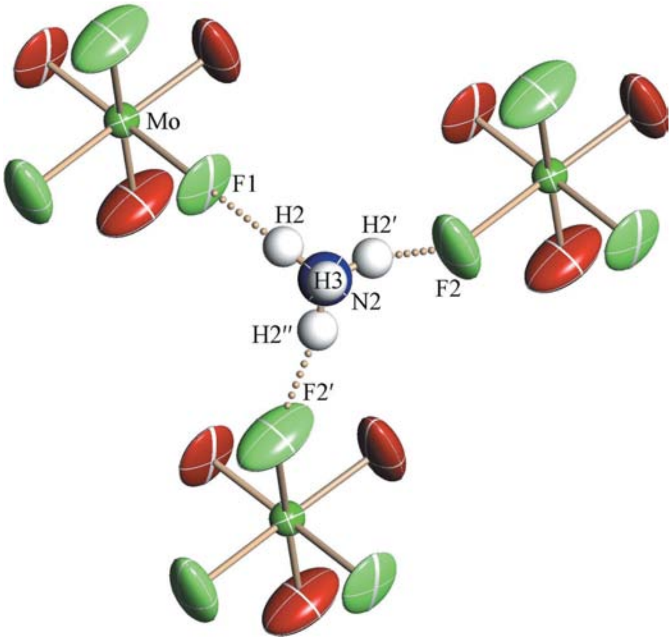

Figure 4
A fragment of the equilibrium structure of $(NH_4)_3MoO_3F_3$ with the scheme of hydrogen bonds N2—H$\cdots$F [the picture is similar for $(NH_4)_3WO_3F_3$].

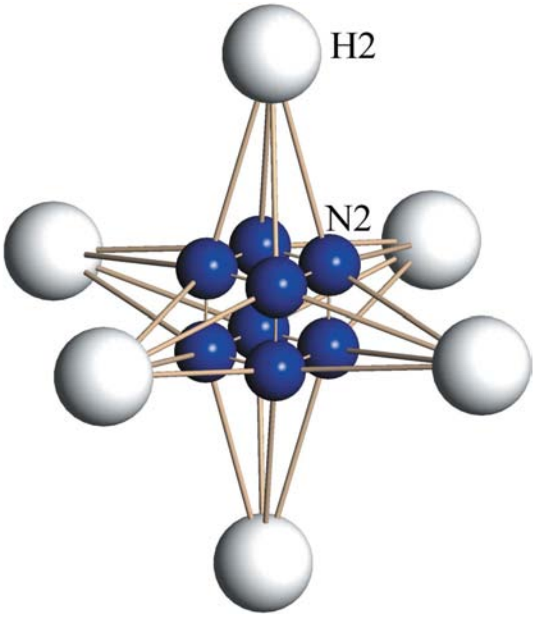

Figure 5
Structure of the disordered $N2H_4$ group. H3 atoms are not shown.

In this respect, the model to calculate the entropy change at the phase transitions in ammonium elpasolites which was suggested by Moriya *et al.* (1977) and based on two configurations of the N2H$_4$ group should be considered as incorrect. Two orientations of NH$_4$ along cubic diagonals would give a cube from H atoms around an N atom, as in the case of the NH$_4$Cl crystal, where the transition between two equivalent states is realised by a 90° rotation of the tetrahedron. In the case of ammonium elpasolites, the octahedron is observed around N2. Two orientations of N2 in the elpasolite structure exclude the existence of hydrogen bonds because of NHF angles less than 117°, while the other models give relatively strong hydrogen bonds. Taking into account eight orientations of the ammonium cation and 48 orientations of the octahedron, the total entropy change must be *R*ln384 at the phase transitions under full ordering of structural units. In fact, it is significantly less: *ca* *R*ln8 for $(NH_4)_3WO_3F_3$ (Flerov *et al.*, 2004) and *ca* *R*ln5 for $(NH_4)_3MoO_3F_3$ (Flerov *et al.*, 2008).

Most likely, ammonium cations and octahedra do not move so independently, but form domains (Fig. 3). The temperature dependence of the second moment (S_2) of ^{19}F NMR spectra for $(NH_4)_3WO_3F_3$ was published (Voit *et al.*, 2006). This S_2/T dependence showed the transition from reorientation motions of octahedral anions at room temperature to a rigid lattice at lower temperature. The absence of a plateau on the S_2/T curve at the lowest temperature of the experiment (135 K, which is lower than the temperature of phase transitions) meant that reorientations were not ‘frozen’ completely.

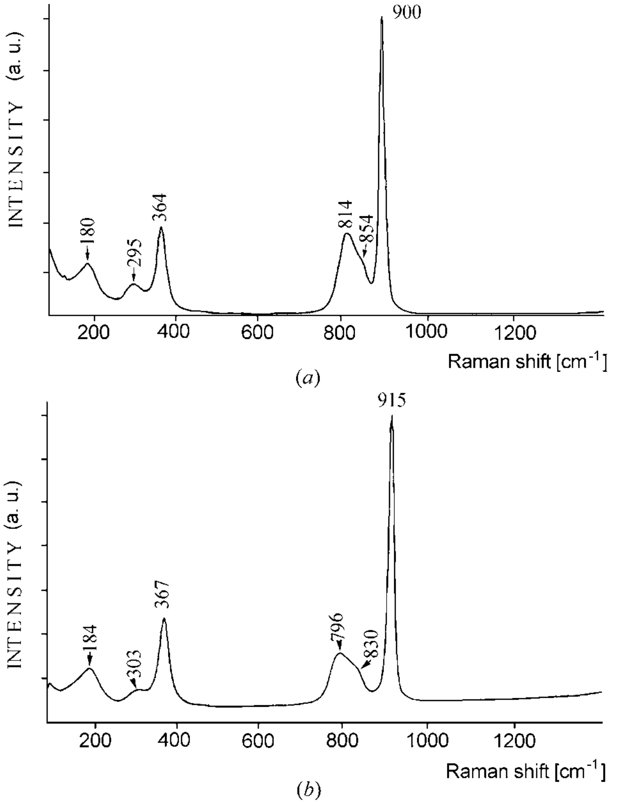

Figure 6
Raman spectra of (*a*) $(NH_4)_3MoO_3F_3$ and (*b*) $(NH_4)_3WO_3F_3$ at room temperature.

To explain the observed entropy change during the phase transitions, it is necessary to determine the crystal structures of $(NH_4)_3MO_3F_3$ low-temperature phases. We failed in carrying out these structural determinations since the crystals changed into thier polydomain state. It should be noted that no reliable data concerning the low-temperature crystal structures of ammonium elpasolites are published. It is clear that phase transitions in ammonium oxofluoromolybdate and oxofluorotungstate are connected with dynamic changes, which are somewhat different for these two complexes (according to their values of entropy changes at phase transitions) and which are reflected in their vibrational spectra.

3.2. Vibrational spectra

It should be emphasized that there is a contradiction in the interpretation of vibrational spectra of $[MO_3F_3]^{n-}$ species reported in the literature. It is considered that the *cis* arrangement of three O atoms (1,2,3 configuration or *fac* structure of C_{3v} symmetry) is preferable. It allows equal sharing of the metal *d* orbitals with the oxygen p_π orbitals in accordance with Griffith & Wickins (1968), Griffith (1969), Atovmjan & Poray-Koshits (1969) and Mattes & Mennemann (1977). Actually, the facial geometry of the $[MO_3F_3]^{n-}$ anion ($M = d^0$ transition metal) has been observed for $[MoO_3F_3]^{3-}$ in the ordered structure of $Na_3MoO_3F_3$ (Brink *et al.*, 2003), for $[WO_3F_3]^{3-}$ as a fragment of the ordered crystal structure of $Pb_5W_3O_9F_{10}$ (Abrahams *et al.*, 1987) and for ordered $[OsO_3F_3]^-$ (Gerken *et al.*, 2000). Three M—O distances in these structures are equal to each other and consistent with the C_{3v} symmetry of the pseudo-octahedral anion. In this case, two bands (both are Raman and IR active) must represent the symmetric and antisymmetric stretching modes of the MO_3 unit, as confirmed by the vibrational spectra and density functional theory (DFT) calculations of $[OsO_3F_3]^-$ species (Gerken *et al.*, 2000).

However, the vibrational spectra of oxofluorometallates $[MO_3F_3]^{3-}$ (M = Mo, W) which crystallizae in the elpasolite-type structure were assigned to the *mer* isomer of C_{2v} symmetry (Pausewang & Rüdorff, 1969; Dehnicke *et al.*, 1969). The same assignment has been made for $[ReO_3F_3]^{2-}$ (Kuhlmann & Sawodny, 1977). The vibrational spectra (IR and Raman) of these species contained three bands in the range of M—O stretches, which were believed to be consistent with the C_{2v} symmetry. Our DFT calculations of both $[WO_3F_3]^{3-}$ configurations showed that the *mer* isomer is 80.8 kJ mol^{-1} higher in energy than the *fac* isomer (Voit *et al.*, 2006), so the latter is preferable in full accordance with our structural determinations of $(NH_4)_3WO_3F_3$. The presence of three bands in the room-temperature Raman spectra of $(NH_4)_3MoO_3F_3$ and $(NH_4)_3WO_3F_3$ (Fig. 6) can be explained by the real anionic geometry, including two short and one longer M—O distances. Correspondingly, three observed bands can be assigned to symmetric and asymmetric stretches of MO_2 and to the *A*1 mode of M—O. The observed IR spectrum of

$(NH_4)_3WO_3F_3$ contains a very broad band extending from 650 to 900 cm^{-1} (Voit *et al.*, 2006). Its computer simulation shows at least three components in this range. The range is *ca* 100 cm^{-1} broader than that of $(NH_4)_3MoO_3F_3$ which indicates the more disordered structure of $(NH_4)_3WO_3F_3$. After the phase transition, the tungsten anion is partially ordered so the more complicated fine structure of the Raman spectra is displayed. The observed changes in the Raman spectra under cooling were presented (Krylov *et al.*, 2006). We supposed (Voit *et al.*, 2006) the intraspheric disorder of $[WO_3F_3]^{3-}$ in addition to its dynamic reorientation as a rigid unit.

4. Conclusions

For the first time, using common X-ray diffraction, we succeeded in ordering the O and F atoms of the extremely disordered kaleidoscopic structure of ammonium oxofluoroelpasolites. Differently oriented octahedra and ammonium cations form domains of lower symmetry than the structure as a whole, which is a consequence of the strong dynamic orientational disorder of the structural units in $(NH_4)_3MoO_3F_3$ and $(NH_4)_3WO_3F_3$. The central atom (Mo or W) as well as the N2 atom are dynamically disordered in the cubic lattice occupying the 32(*f*) position. Their displacement from symmetry centers indicates the O/F ordering on a local scale. The character of the observed vibration spectra of the disordered *fac*-$[MO_3F_3]^{3-}$ species can be explained from their true geometry, which is rather far from C_{3v}.

We thank V. Ya. Kavun for ^1H and ^{19}F NMR spectra of $(NH_4)_3WO_3F_3$ and V. A. Davydov for registration of vibrational spectra of the compounds examined.

References

Abrahams, S. C., Marsh, P. & Ravez, J. (1987). *J. Chem. Phys.* **87**, 6012–6020.

Atovmjan, L. O. & Poray-Koshits, M. A. (1969). *Zh. Strukt. Khim.* **10**, 853–858.

Brink, F. J., Norén, L., Goossens, D. J., Withers, R. L., Liu, Y. & Xu, C.-N. (2003). *J. Solid State Chem.* **174**, 450–458.

Bruker (1998*a*). *SMART*. Bruker AXS Inc., Madison, Wisconsin, USA.

Bruker (1998*b*). *SAINT-Plus*, Versions 5.0. Bruker AXS Inc., Madison, Wisconsin, USA.

Dehnicke, K., Pausewang, G. & Rüdorff, W. (1969). *Z. Anorg. Allg. Chem.* **366**, 64–72.

Flerov, I. N., Gorev, M. V., Fokina, V. D., Bovina, A. F. & Laptash, N. M. (2004). *Fiz. Tverd. Tela*, **46**, 888–894.

Flerov, I. N., Fokina, V. D., Bovina, A. F., Bogdanov, E. V., Molokeev, M. S., Kocharova, A. G., Pogorel'tsev, E. I. & Laptash, N. M. (2008). *Russ. Phys. Solid State*, **50**, 515–524 [translated from *Fiz. Tverch. Tela.* **50**, 497–506].

Gerken, M., Dixon, D. A. & Schrobilgen, G. J. (2000). *Inorg. Chem.* **39**, 4244–4255.

Griffith, W. P. (1969). *J. Chem. Soc. A*, pp. 211–218.

Griffith, W. P. & Wickins, T. D. (1968). *J. Chem. Soc. A*, pp. 400–404.

Heier, K. R., Norquist, A. J., Halasyamani, P. S., Duarte, A., Stern, C. L. & Poeppelmeier, K. R. (1999). *Inorg. Chem.* **38**, 762–767.

Krahl, T., Ahrens, M., Scholz, G., Heidemann, D. & Kemnitz, E. (2008). *Inorg. Chem.* **47**, 663–670.

Krylov, A. S., Gerasimova, Yu. V., Vtyurin, A. N., Fokina, V. D., Laptash, N. M. & Voyt, E. I. (2006). *Phys. Status Solidi B*, **243**, 435–441.

Kuhlmann, W. & Sawodny, W. J. (1977). *J. Fluorine Chem.* **9**, 341–357.

Maggard, P. A., Nault, T. S., Stern, C. L. & Poeppelmeier, K. R. (2003). *J. Solid State Chem.* **175**, 27–33.

Marignac, M. C. (1862). *C. R. Acad. Sci* **55**, 888–892.

Marignac, M. C. (1863). *Ann. Chim. Phys.* **69**, 61–86.

Mattes, R. & Mennemann, K. (1977). *Z. Anorg. Allg. Chem.* **437**, 175–182.

Moriya, K., Matsuo, T., Suga, H. & Seki, S. (1977). *Bull. Chem. Soc. Japan.* **50**, 1920–1926.

Paasch, M., McIntyre, G. J., Reehuis, M., Sonntag, R. & Loidl, A. (1996). *Z. Phys. B*, **99**, 339–344.

Pauling, L. (1924). *J Am. Chem. Soc.* **46**, 2738–2751.

Pausewang, G. & Rüdorff, W. (1969). *Z. Anorg. Allg. Chem.* **364**, 69–87.

Schwarzman, S. (1964). *Z. Kristallogr.* **120**, 286–312.

Seymour, R. S. & Pryor, A. W. (1970). *Acta Cryst.* B**26**, 1487–1491.

Sheldrick, G. M. (2008). *Acta Cryst.* A**64**, 112–122.

Udovenko, A. A., Laptash, N. M. & Maslennikova, I. G. (2003). *J. Fluorine Chem.* **124**, 5–15.

Voit, E. I., Voit, A. I., Mashkovsky, A. A., Laptash, N. M. & Kavun, V. Ya. (2006). *Russ. J. Struct. Chem.* **47**, 642–650 (translated from (2006). *Zh. Strukt. Khim.* **47**, 661–669.

Withers, R. L., Brink, F. J., Liu, Y. & Norén, L. (2007). *Polyhedron*, **26**, 290–299.

Withers, R. L., Welberry, T. R., Brink, F. J. & Norén, L. (2003). *J. Solid State Chem.* **170**, 211–220.